

# Magnesium-based materials in orthopaedics: material properties and animal models

Xirui Jing<sup>1</sup>, Qiuyue Ding<sup>1</sup>, Qinxue Wu<sup>2</sup>, Weijie Su<sup>1</sup>, Keda Yu<sup>1</sup>, Yanlin Su<sup>1</sup>, Bing Ye<sup>1</sup>, Qing Gao<sup>1</sup>, Tingfang Sun<sup>1</sup>, Xiaodong Guo<sup>1,\*</sup>

## Key Words:

animal models; bone regeneration; magnesium; magnesium alloy; tissue engineering

## From the Contents

<b>Introduction</b>	<b>197</b>
<b>Magnesium Homeostasis and Its Effects In Vivo</b>	<b>199</b>
<b>Properties of Magnesium-Based Materials</b>	<b>200</b>
<b>Methods and Evaluation of Common Animal Models for Magnesium-Based Implants</b>	<b>200</b>
<b>Animal Models for Research into Magnesium-Based Materials</b>	<b>204</b>
<b>Summary and Outlook</b>	<b>208</b>

## ABSTRACT

As a new generation of medical metal materials, degradable magnesium-based materials have excellent mechanical properties and osteogenic promoting ability, making them promising materials for the treatment of refractory bone diseases. Animal models can be used to understand and evaluate the performance of materials in complex physiological environments, providing relevant data for preclinical evaluation of implants and laying the foundation for subsequent clinical studies. To date, many researchers have studied the biocompatibility, degradability and osteogenesis of magnesium-based materials, but there is a lack of review regarding the effects of magnesium-based materials in vivo. In view of the growing interest in these materials, this review briefly describes the properties of magnesium-based materials and focuses on the safety and efficacy of magnesium-based materials in vivo. Various animal models including rats, rabbits, dogs and pigs are covered to better understand and evaluate the progress and future of magnesium-based materials. This literature analysis reveals that the magnesium-based materials have good biocompatibility and osteogenic activity, thus causing no adverse reaction around the implants in vivo, and that they exhibit a beneficial effect in the process of bone repair. In addition, the degradation rate in vivo can also be improved by means of alloying and coating. These encouraging results show a promising future for the use of magnesium-based materials in musculoskeletal disorders.

## \*Corresponding author:

Xiaodong Guo,  
xiaodongguo@hust.edu.cn.

<http://doi.org/10.12336/biomatertransl.2021.03.004>

## How to cite this article:

Jing, X.; Ding, Q.; Wu, Q.; Su, W.; Yu, K.; Su, Y.; Ye, B.; Gao, Q.; Sun, T.; Guo, X. Magnesium-based materials in orthopaedics: material properties and animal models. *Biomater Transl.* 2021, 2(3), 197-213.



## Introduction

Musculoskeletal disorders are one of the most common human health problems, which greatly affect patients' quality of life.<sup>1</sup> Due to the increase in global aging, musculoskeletal disorders have attracted much attention. As one of the most commonly-used medical devices for treatment of bone-related diseases, biomaterials play an irreplaceable role in their treatment. To date, metal implants, represented by titanium and stainless steel, have been widely used in the clinic.<sup>2</sup> These implants have good biocompatibility and mechanical properties and meet the clinical needs, but they still have certain limitations such as stress shielding, which can impair the bone repair process, especially in patients with osteoporosis.<sup>3</sup> In addition, due to the non-

biodegradable nature of these implants, a second operation is often required to remove them in order to avoid adverse effects caused by the long-term presence of the implants, which creates an unnecessary burden on patients. Therefore, the development of new biodegradable implants that can overcome the above problems is a promising direction in the field of bone tissue engineering.

As a newly-developed orthopaedic material, biodegradable polymers have received a lot of attention. For example, implants made from polylactide, polyglycolide and co-polymers are degradable and have mechanical properties close to those of cancellous bone. Some biodegradable polymers have been approved by the U.S. Food and Drug Administration for use in orthopaedic applications.<sup>4,5</sup> However, due to their inadequate

mechanical properties, polymer products have the risk of surgical failure and are limited to non-weight-bearing parts.<sup>4,6</sup> By-products produced during the degradation process can affect the local microenvironment and induce inflammatory responses, which can restrict the resulting bone regeneration.<sup>7</sup> According to a previous report, complete degradation of polymer products does not promote bone ingrowth.<sup>8</sup>

Although biodegradable polymers have been widely used in orthopaedics, their deficiencies limit their use in refractory diseases such as osteoporotic fractures, atypical femoral fractures, and other fractures. Therefore, there is still a need to find biodegradable implants that can overcome these problems.<sup>9,10</sup> Magnesium (Mg) is one of the common elements

found in nature and is abundant in the human body. At present, the development of biomaterials based on Mg has attracted the attention of researchers (Figure 1).<sup>11-21</sup> Mg-based implants are biodegradable materials with good biocompatibility which are far less likely to induce adverse reactions after implantation.<sup>22</sup> Mg has an excellent Young's modulus, which is close to that of natural cortical bone, thus avoiding stress-shielding.<sup>23</sup> Evidence has shown that Mg released during the degradation process promotes bone repair and accelerates bone healing in a number of ways, so it has a greater advantage in the treatment of refractory bone diseases compared to other degradable implants.<sup>24,25</sup> Mg-based implants may be able to address the shortcomings of current commercially-available orthopaedic implants.

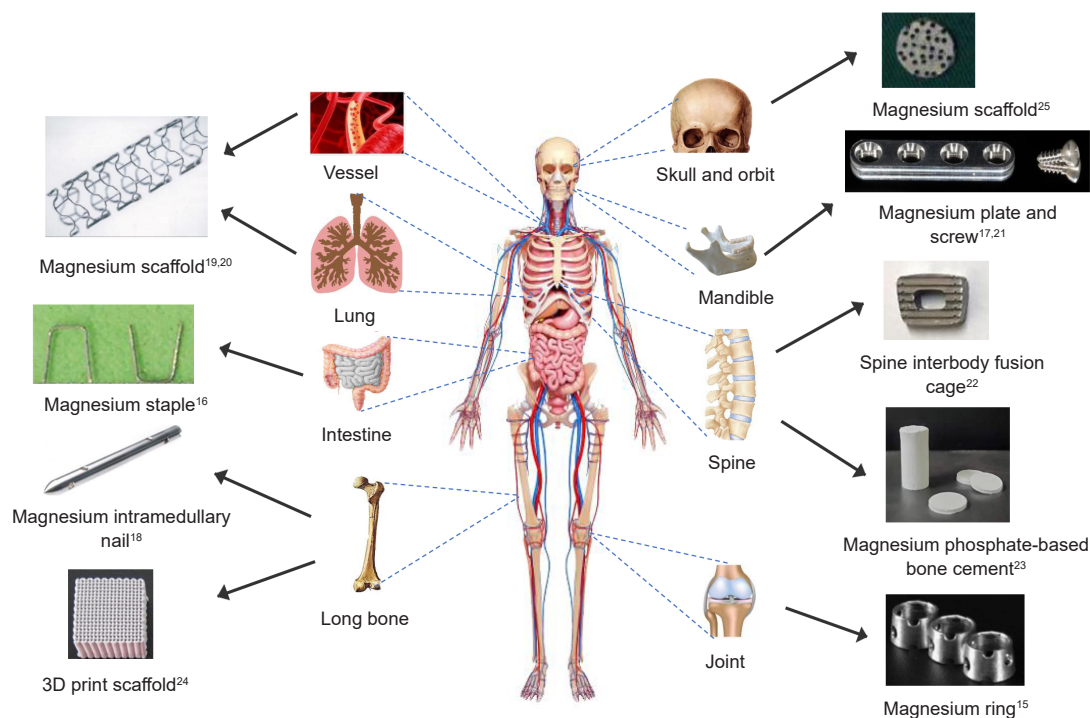


Figure 1. Some representative magnesium-based implants. Adapted from Farraro et al.<sup>11-21</sup>

Although Mg-based implants have shown great potential in the treatment of musculoskeletal diseases, there are still problems that need to be addressed. After implantation, Mg-based implants exhibit high corrosion sensitivity and non-uniform corrosion behaviour due to the presence of stress and a large number of chloride ions in the physiological environment.<sup>26</sup> Excessive degradation of the materials will release too many ions and excess hydrogen, which will affect the local microenvironment of the implants and cause gas cavity formation.<sup>27,28</sup> In addition, degradation after implantation can also impair the mechanical properties, increasing the risk of losing fixation before fracture healing.<sup>29</sup> Therefore, in order to study the effects of Mg-based implants *in vivo*, it is necessary

to investigate the safety and efficacy of these implants in small and large animal models.

Animal studies of Mg-based implants can provide relevant data for preclinical evaluation of the implants and lay the foundation for subsequent clinical studies. To date, many studies have evaluated the biocompatibility, degradability and osteogenic properties of Mg-based implants *in vivo*.<sup>30-35</sup> A number of factors need to be considered in selecting a specific animal as an experimental model, including animal availability; selection of an animal model that exhibits pathophysiological characteristics similar to humans; the size of the implants, the number of implants in each animal, and the time for observation; the operability of the surgery and the difficulty

1Department of Orthopaedics, Union Hospital, Tongji Medical College, Huazhong University of Science and Technology, Wuhan, Hubei Province, China; 2Department of Clinical Medicine, Hubei Enshi College, Enshi, Hubei Province, China

of obtaining the observation indices.<sup>36, 37</sup> The purpose of this article is to review the current published studies on Mg-based implants *in vivo* to evaluate the safety and efficacy of Mg-based implants. We searched the Web of Science® and PubMed® databases using the following keywords: bone; bone regeneration; magnesium; magnesium alloy; pure magnesium; *in vivo*; animal model; cardiovascular diseases. Searches were performed with different combinations of keywords to obtain more results. Some of the results were excluded based on the title, and then the articles were further screened by reading the abstract, and the articles that did not meet the inclusion criterion (animal models used for Mg-based materials research) were removed. All these searches were performed on PubMed, and Web of Science databases prior to August, 2021.

### Magnesium Homeostasis and Its Effects *In Vivo*

Mg, an essential ion in the human body, is the second most abundant cation in mammalian cells, second only to potassium.<sup>38</sup> Mg plays an important role in supporting and maintaining health and life and is essential in many physiological processes, including enzymatic reactions, cell signal transduction, ion

channel function, cell metabolism and biomolecular stability.<sup>39, 40</sup> Mg homeostasis is a basic requirement for cell growth, differentiation, energy metabolism and cell death, especially in the brain, heart and skeletal muscle.<sup>41</sup> In addition, Mg supplements have been shown to be beneficial for bone repair, coronary heart disease and asthma. Maintaining Mg ion concentrations within an optimal range is therefore critical for normal cell function and disease prevention.<sup>41</sup>

### Magnesium homeostasis *in vivo*

The total Mg content in a healthy adult weighing 70 kg is about 24 g, and 99% of the body's Mg is found in bone, muscle and soft tissue.<sup>42, 43</sup> Most of the Mg in bone is in the form of hydroxyapatite surface substituents. To maintain health, the recommended daily intake of Mg for adults is 300–400 mg (Figure 2).<sup>42, 44, 45</sup> Mg can be absorbed from the intestine and excess Mg is removed from the body in faeces and urine. Therefore, high concentrations of Mg due to degradation of Mg-based implants are permissible as the excess can be transported through the circulatory system to the urinary system and excreted without other adverse effects.<sup>44</sup>

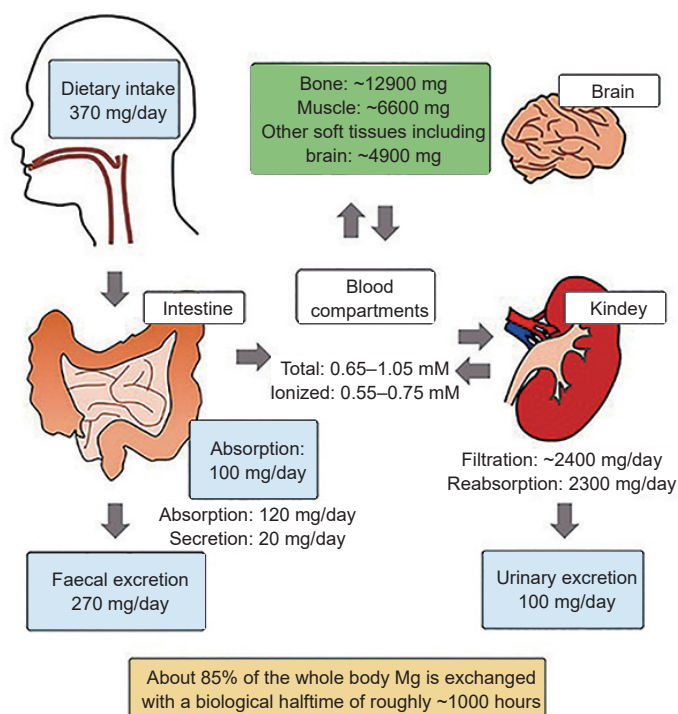


**Figure 2.** Magnesium metabolism of the human body. Reprinted from Yamanaka et al.<sup>45</sup>

### The role of magnesium in bone

Hydroxyapatite is one of the main components of bone, and most of the Mg ions in bone are bound to the surface of crystalline hydroxyapatite. A lack of Mg in hydroxyapatite crystals makes them larger, making bones brittle and more prone to fracture. Moreover, Mg can promote bone formation in more than one way. The ion is beneficial to the proliferation and differentiation of mesenchymal stem cells, and promotes the secretion of vascular endothelial growth factor, a factor associated with angiogenesis, thus speeding up the process of bone regeneration.<sup>46</sup> Mg deficiency increases the number of

osteoclasts, and Mg supplementation attenuates this effect, as a result of which Mg supplementation increases the number of osteoclast precursors.<sup>47, 48</sup> Osteoclast precursor cells are the source of platelet-derived growth factor-BB, which is conducive to the formation of type H vessels in the process of osteogenesis.<sup>49, 50</sup> Mg has an osteoimmunomodulatory effect, promoting the polarisation of macrophages to M2 stage and inhibiting the transformation to M1 stage.<sup>51, 52</sup> M2 macrophages are associated with mineralisation, and increased M2 macrophages are conducive to bone regeneration, while a decrease in M1 macrophages is indicative of the anti-

inflammatory effect of Mg.<sup>53, 54</sup> The periosteum contains a large number of nerves. In the early stage of fracture repair, nerves are the first tissue to regenerate and participate in the fracture repair process.<sup>55</sup> The degradation of Mg implants *in vivo* releases Mg ions, which migrate to the surface of bone where they are picked up by axons. Mg ions entering the axons encourage the axons to release more calcitonin gene-related peptide, which acts on periosteum stem cells to facilitate bone repair.<sup>56</sup>

### The role of magnesium in other tissues

Mg ions are necessary for the heart to function properly, playing an important role in the second and third stages of cardiac action potential by affecting potassium channels and calcium channels.<sup>41</sup> As a natural calcium antagonist, Mg participates in cardiac activation–contraction coupling by competing with calcium to bind proteins and calcium transporters.<sup>57</sup> In addition, Mg has been reported to have a substantial vasodilation effect, the possible mechanism of which is through regulation of nitric oxide synthesis, although its induction of vasodilation has also been reported independent of nitric oxide.<sup>58, 59</sup>

The lack of research on Mg in the lung has led to a poor understanding of the mechanisms by which Mg plays a role in lung function, and most hypotheses are based on other tissues and cells. Like most vasodilators, Mg induces bronchial dilation, possibly by inhibiting the release of acetylcholine and histamine.<sup>60, 61</sup> Declines in Mg levels have been reported in asthmatic patients, suggesting a possible link between Mg level and asthma.<sup>62, 63</sup> In addition, low Mg is associated with inflammation, and due to its anti-inflammatory effects, Mg supplementation may reduce the inflammatory response in

some lung diseases, such as chronic obstructive pulmonary disease.<sup>64, 65</sup>

### Properties of Magnesium-Based Materials

Metal implants such as stainless steel, titanium alloy, and cobalt chromium alloy are widely used in the biomedical field.<sup>66, 67</sup> These metal implants have been recognised in the field of orthopaedics for their excellent mechanical strength and good biocompatibility. However, these implants still have disadvantages, including: 1) traditional metal implants are non-degradable and often require a second surgical removal; and 2) stress shielding, which affects bone repair, especially in osteoporotic fractures.<sup>3</sup> Mg and its alloys have been highlighted for their ability to overcome these problems due to their degradability and excellent mechanical properties.

### Mechanical properties

Mg is one of the lightest metals and its alloys (weighing 1.7–1.9 g/cm<sup>3</sup>) have a mechanical strength similar to cortical bone.<sup>68, 69</sup> Although their degradability is similar, degradable biopolymers often have poor mechanical properties, and Mg-based implants have better mechanical strength than biodegradable biopolymers.<sup>2</sup> Compared with other metal implants, Mg-based implants have a similar elastic modulus to cortical bone, thus minimising stress blocking.<sup>69, 70</sup> In the process of bone regeneration, the mechanical properties of the healing bone gradually improve as the repair process proceeds, thus the mechanical strength of an ideal bone implant material should gradually reduce in parallel with the healing process<sup>22</sup> (Table 1). The use of Mg-based implants provides a great opportunity to meet this requirement.<sup>71</sup>

**Table 1. Mechanical properties of various metallic implants compared with natural bone.**

Property	Natural bone	Magnesium alloys	Titanium alloys	Stainless steels
Density (g/cm <sup>3</sup> )	1.8–2.1	1.74–2.0	4.4–4.5	7.9–8.1
Elastic modulus (GPa)	3–20	41–45	110–117	189–205
Yield strength (MPa)	130–180	85–190	758–1117	170–310

Note: Data are sourced from Chakraborty Banerjee et al.<sup>22</sup>

### Degradation properties

The biodegradability of Mg-based implants is one of the reasons they have attracted the attention of researchers. Corrosion of Mg in aqueous solution is an electrochemical phenomenon which occurs by reaction with water to produce Mg hydroxide and hydrogen gas.<sup>72</sup> Hydrogen is an antioxidant and the hydrogen produced by the degradation of Mg implants can reduce cell damage caused by oxidative stress.<sup>73</sup> Meanwhile Mg hydroxide produced by the degradation of Mg-based implants can cover the surface of the implants, forming a protective layer and reducing the corrosion of Mg.<sup>74</sup> In the physiological environment, due to the presence of high concentrations of chloride, magnesium hydroxide is converted to magnesium chloride, which is highly soluble and accelerates the corrosion of Mg-based implants, resulting in a local increase in the pH value.<sup>28</sup> Other components of the physiological environment also have different effects on Mg implants, including calcium ions, phosphate ions, and proteins.<sup>75, 76</sup>

Compared with biodegradable biopolymers and biodegradable bioceramics, Mg and its alloys have better mechanical properties.<sup>2</sup> During the degradation process, the mechanical properties of Mg alloy implants will decrease, rapid corrosion will damage the mechanical integrity of the Mg implants and release a large amount of hydrogen and hydroxide ions in a short time, although these products can be exchanged rapidly through local tissues.<sup>77</sup> However, too fast degradation will still damage the stability of the local microenvironment.<sup>35, 78</sup> Methods including purification, surface modification and alloying have been adopted to improve the spatio-temporal complementarity between bone regeneration and implant degradation.<sup>79</sup>

### Methods and Evaluation of Common Animal Models for Magnesium-Based Implants

The bone defect model is a commonly-used model to evaluate the osteogenic effect of implants in musculoskeletal diseases (Figure

3).<sup>80</sup> Currently, many animal models have been developed for evaluating bone implants, among which skull defects, long bone defects, partial cortical defects and cancellous defects are the most commonly used.<sup>81</sup> Whichever model is chosen, consideration

should be given to the size of the defect and the type of material to be implanted. We summarise the common bone defect models used at present, and briefly describe the modelling methods and points for attention of different animal models.

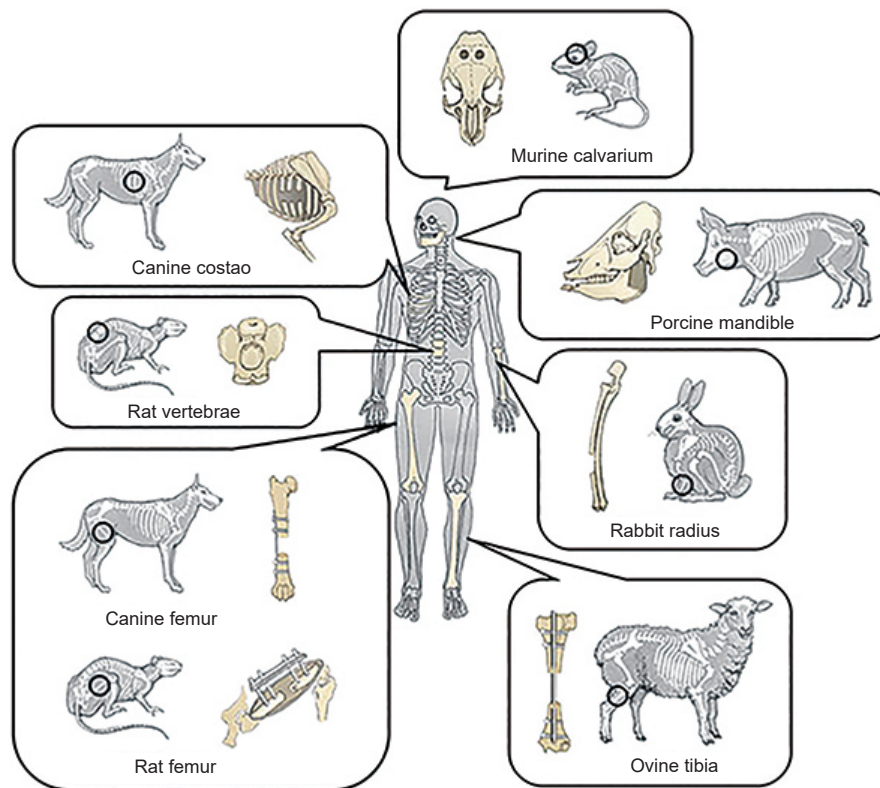


**Figure 3.** Common animal models used for bone regeneration. Reprinted from Taguchi and Lopez.<sup>80</sup>

### Skull defect model

The skull defect model is one of the most commonly-used models of bone defect, and the rabbit and rat are usually the first choice for the skull defect model.<sup>81,82</sup> This model has been well studied and widely accepted and has several advantages, including: 1) The skull is a plate-like structure in which a uniform circular defect can be surgically created for radiological and histological purposes. 2) The skull defect model is easy to prepare and the specimen is easy to obtain. 3) The model has been fully studied. 4) It is a relatively economical model.<sup>83</sup> Due to the inability to assess the performance of implants under physiological mechanical loads, the applicability of skull defect models to some implants may be limited. Nevertheless the critical size defect model of the skull is simple to create: an anteroposterior midline skin incision is made at the top of the skull (rabbit: 4–5 cm long, Sprague-Dawley rat: 1–2 cm long), and the soft tissue and periosteum are separated layer by layer to expose the skull. In general, for Sprague-Dawley rats, two 5 mm diameter defects are created using a trephine on either side of the midline, between the transverse bone sutures, or an 8 mm diameter defect is produced on the midline.<sup>83–85</sup> During the process of drilling, the defect should be continuously irrigated with saline to avoid causing damage to the surrounding tissues due to the high temperature, and the osteotomy depth should

be periodically examined to avoid puncturing the dura mater. If the full thickness of the bone plate is found to be penetrated, the dura mater is often already involved, which may cause an intracranial hematoma. After the implant is placed into the defect, the periosteum and subcutaneous tissue are closed. If a hematoma appears after surgery, drainage can be achieved by cutting several skin sutures.<sup>83,86</sup>

To create a rat model of infected cranial defects, 3 or 4 mm full-thickness skin defects are usually created in Sprague-Dawley rats.<sup>87</sup> After that, a resorbable collagen plug which has been pre-soaked with pathogenic bacteria is placed in the defect. *Staphylococcus aureus* or methicillin-resistant *S. aureus* ( $1 \times 10^7$  colony-forming units suspended in 100  $\mu$ L sterile normal saline) are usually used, and after the material is placed in position, the periosteum and skin are closed.<sup>87</sup> Debridement is then performed one week after the first operation, involving re-exposure of the skull from the original incision, removal of all nonviable tissue, exposure of the bone defect, implantation of the material, and suturing of the incision layer by layer<sup>88</sup> (**Figure 4**). Postoperatively, by paying close attention to basic physical signs in the experimental animals, systemic infections can be detected in a timely manner, such as by changes in body temperature and weight, and swelling which is likely to be seen at the top of the skull.

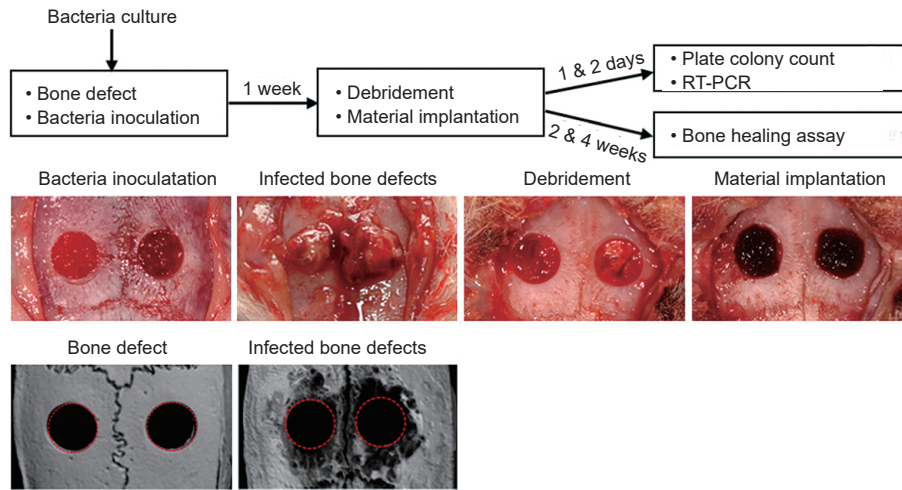


**Figure 4.** Creation of infected cranial defects. Adapted from Dong et al.<sup>88</sup> Copyright 2017, with permission from Elsevier. RT-PCR: real-time polymerase chain reaction.

**Long bone defect models**

Long bone defect models can be used to evaluate material performance under physiological loading, which is closer to clinical conditions, although the weight on the limbs in animals is still not the same as in humans since it gets distributed over a larger number of limbs. This model has been established in a number of species, including mice, dogs, sheep, goats, pigs, etc.<sup>89, 90</sup> (Figure 5). Dogs have been the traditional model used in orthopaedic research, but their use has declined due to public concerns; pigs require careful handling which discourages their use; consequently sheep are the most commonly-used model for long-bone segmental defects. Mature sheep have similar body weight to adult humans and also have similar metabolic and bone remodelling rates to humans, and so are

more relevant to clinical practice.<sup>91</sup> Many segmental defects of long bones have been reported; taking sheep mid-diaphyseal segmental tibial defects as an example, skin and soft tissue are cut open to expose the tibia and a dynamic compression plate is temporarily fixed with two screws. After drilling the screw holes, the defect and osteotomy line are exposed. The osteotomy is then performed to remove the bone segment and then plates and screws are used for fixation. An implant is placed and sutures are used to close the wound. The tibia is the most commonly-used anatomical site in sheep models, other sites used for segmental long bone defects include the proximal third of the tibia, the femoral neck and the metatarsus.<sup>92</sup> Typically, critical-sized defects of the tibia are 2 to 2.5 times the diameter of the bone.<sup>93</sup>

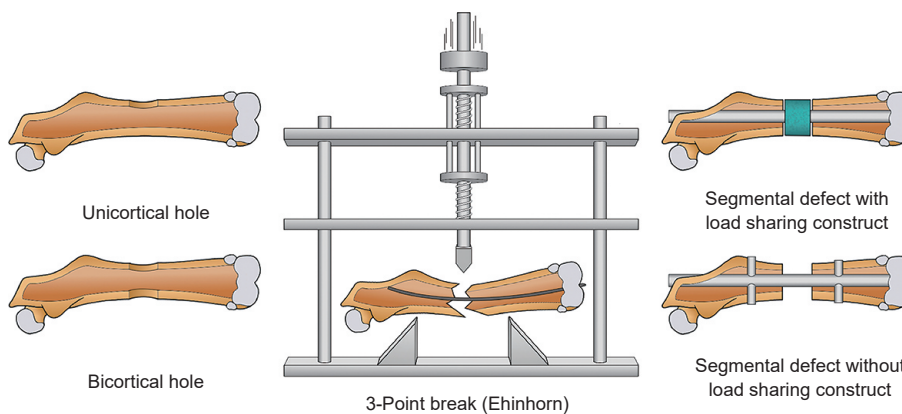


**Figure 5.** Illustration of bone healing models in the femoral diaphysis. Reprinted from Gunderson et al.<sup>90</sup> Copyright 2020, with permission from Elsevier.

The type of internal fixation used for segmental bone defects affects the quality of bone healing.<sup>94, 95</sup> Bone plates and intramedullary nails are commonly used to stabilise long bone defects and simulate the clinical environment (Figure 6). However, if the fixation is too rigid, the repair may be compromised.<sup>95, 96</sup> External fixation combined with mesh implants is a possible alternative to internal fixation, as it reduces the biological response at the defect site.<sup>93</sup> The model

of bone tissue infection has laid a stable foundation for the pathogenesis and prevention of osteomyelitis. Long bone osteomyelitis can be modelled by intramedullary injection of pathogenic bacteria or by preconditioning the implant with pathogenic bacteria<sup>97, 98</sup> (Figure 7). The local soft tissue and the activity of the animal should be observed regularly after operation, and the body temperature and weight of the animal should be measured.

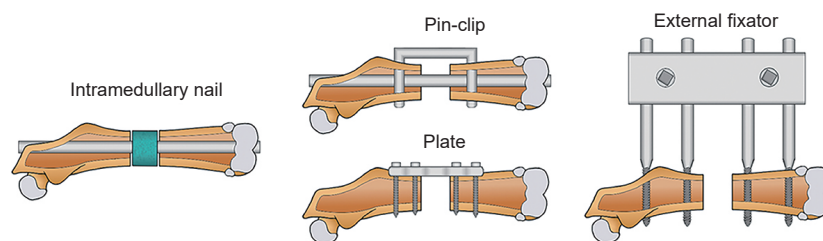


**Figure 6.** Fixation types for a segmental femoral defect. Reprinted from Gunderson et al.<sup>90</sup> Copyright 2020, with permission from Elsevier.

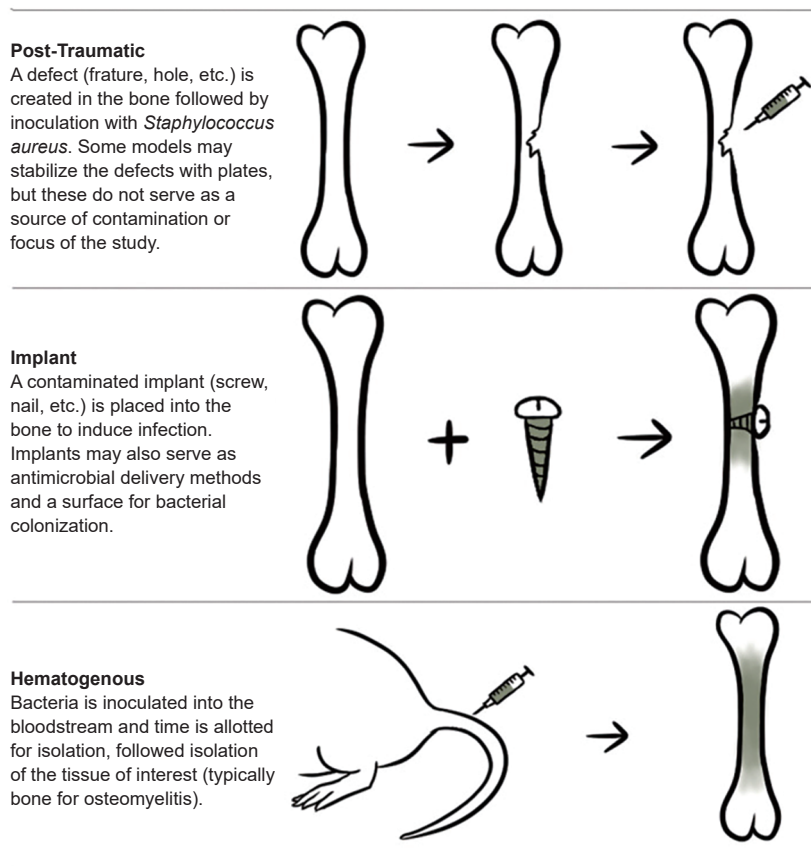


**Figure 7.** Methods used to induce osteomyelitis in animal models. Reprinted from Roux et al.<sup>98</sup>

### Craniofacial bone defect model

Unlike most bones in the body that are derived from the mesoderm, the maxillofacial bones develop from neural crest tissue.<sup>99,100</sup> Moreover, due to the differences in mechanical load and blood supply, models of skull defects and long bone defects are not suitable for evaluating bone repair of a maxillofacial bone defect.<sup>101</sup> To address this problem a rat model of a maxillofacial borehole bone defect has been introduced.<sup>101</sup> The skin and the lower soft tissue are cut in parallel at 0.5 mm above the lower margin of the mandible to expose the bone tissue. A flat-end cylinder diamond burr is then used to construct burr hole defects on the surface of the bone tissue. After that, the subcutaneous tissue is repositioned and the skin is sutured. Intraoperative injury to the parotid gland, parotid duct, masseter muscle and facial nerve should be avoided.

### Common carotid artery lateral aneurysm model

The use of Mg alloy scaffolds is a promising method for the

treatment of aneurysms.<sup>15, 102</sup> The lateral aneurysm model can be used to evaluate the efficacy of implants in the treatment of aneurysm occlusion, and a lateral aneurysm model has been established in rabbits.<sup>103</sup> One month before surgery, the left common carotid artery is ligated to thicken the right common carotid artery, which is then conducive to the generation of aneurysms. Rabbits are anaesthetised and fixed in the supine position. After full disinfection, a horizontal skin incision is made below the thyroid cartilage and slightly to the right of the midline. Then, the subcutaneous tissue is separated layer by layer to expose the right external jugular vein. The venous proximal and distal parts are ligated and a venous pouch is clipped. The right anterior cervical muscle group is then dissected to reveal the right common carotid artery, and haemostatic forceps are used to temporarily clamp the proximal and distal sides. An incision is made between the haemostatic forceps, and the right common carotid artery is anastomosed with the venous pouch. Finally the clamp is loosened to allow

the venous pouch to fill while keeping a close watch on blood flow.

### Evaluation of animal models for bone defects

Radiological assessment is one of the most commonly-used methods for the assessment of orthopaedic diseases.<sup>104, 105</sup> Dual energy X-ray absorptiometry is the gold standard for the diagnosis of osteopenia and osteoporosis and a medium predictor of fracture risk, which can be used for the overall evaluation of bone healing.<sup>106-108</sup> Micro-computed tomography (CT), which uses X-ray attenuation data collected from multiple perspectives to reconstruct three-dimensional images of samples representing the spatial distribution of material density, has become the gold standard for evaluating bone morphology and microstructure in animal models *in vitro*.<sup>109</sup> Micro-CT has many advantages for evaluating the bone mass and morphology of specimens, for example, it allows direct three-dimensional measurement of trabecular morphology, such as trabecular thickness and separation. Bone morphology can be evaluated in a non-destructive manner by a micro-CT scan, and the sample can then be used for other tests.<sup>110, 111</sup>

Staining histological slides for orthopaedic studies provides the possibility of visualising inflammatory responses and healing responses at the defect site.<sup>112</sup> Stains commonly used in orthopaedics include haematoxylin and eosin, Masson's trichrome, Safranin O-fast green, and toluidine blue.<sup>113-116</sup> Classical haematoxylin and eosin staining is a routine pathological stain, which can be used to judge biocompatibility by evaluating the inflammatory response; however haematoxylin and eosin stains all bone in a purple-pink colour, so it does not allow for obvious identification of new bone and pre-existing bone within the defect site.<sup>117</sup> In order to identify the formation of new bone at the defect site, other supplementary stains are often needed. For example, Masson's trichrome stains osteoid orange-red or red, and mineralised bone blue. Other special stains include terminal deoxynucleotidyl transferase-mediated dUTP nick-end labelling staining, which can be used to assess apoptosis, and tartrate-resistant acid phosphatase, which is used to label osteoclasts.<sup>118</sup>

## Animal Models for Research into Magnesium-Based Materials

### Animal models for research into the use of magnesium-based materials in orthopaedics

#### Rat model studies

As one of the methods to improve the corrosion performance of implants, the use of high-purity Mg as the implant material shows promise. Pure Mg implants have been extensively studied in rat models. Hamushan et al.<sup>119</sup> created a distraction osteogenesis model in Sprague-Dawley rats to evaluate the effect and mechanism of high-purity Mg (Hp Mg) pins on osteogenesis. Mg implantation significantly improved the quantity and quality of healed bone tissue, and showed a faster consolidation speed during the repair process. The consolidation process was almost completed at 9 weeks and had a higher ultimate load and energy to failure in the mechanical test. Due to its high purity, the Mg implants showed stable

degradability in experiments, providing continuous guidance. Using RNA-sequencing analysis and other methods, the authors found that Mg promotes osteogenesis by regulating patched 1 protein, thus activating Hedgehog-alternative Wnt signalling.

Zhang et al.<sup>56</sup> implanted a 99.99%-pure Mg rod in a Sprague-Dawley rat nonfractured femur model. Two weeks after surgery, a significant increase in Mg concentration was found in the cortical bone and the bone-periosteum junction of the femur implanted with Mg, revealing a remarkably higher Mg concentration in the cortical bone and bone-periosteum junction of the Mg-implanted femora and a great deal of new bone formation in cortical bone. A high concentration of calcitonin gene-related peptide was observed in the peripheral cortical bone implanted with Mg by immunofluorescence staining. When the periosteum was removed pre-implantation, the formation of new bone in this area was significantly reduced. The authors suggest that Mg promotes the secretion of calcitonin gene-related peptide by axons on the bone surface to induce new bone formation, which is eliminated by periosteum removal.

Periprosthetic infections are one of the most common complications in orthopaedics. Prolonged antimicrobial treatment, implant removal, and surgical revision is the conventional way to treat periprosthetic infections, but this often places an unnecessary burden on patients.<sup>120</sup> Robinson et al.<sup>121</sup> reported that Mg has antibacterial activity *in vitro*, which may be due to the local alkaline environment caused by Mg degradation. To evaluate the antibacterial activity of pure Mg *in vivo*, Li et al.<sup>122</sup> implanted pure Mg intramedullary nails in 5-month-old Sprague-Dawley rats. Mg implantation reduced the bone destruction caused by infection and effectively protected bone and surrounding tissues from methicillin-resistant *S. aureus* infection. The bone around the implant was evaluated by micro-CT, and the Mg implant group had higher bone mineral density, bone mineral content, and bone volume/tissue volume, as well as lower total porosity and number of pores than the control group. This suggested that pure Mg intramedullary nails could prevent the destruction of infected bone and promote the formation of bone around the implant.

Compared with long bones, craniofacial bone has a different embryonic origin and growth process, and the biological characteristics of the periosteum of craniofacial bone are also different from those of long bone. In order to identify the osteogenic effect of Mg on mandibular alveolar bone, He et al.<sup>123</sup> implanted pure Mg in the sockets after extraction of rat mandibular incisors. At 2 weeks postoperatively, the concentration of Mg around the alveolar bone was significantly higher than that in the control group, and the Mg appeared beneficial for the repair of cortical and trabecular bone in the alveolar bone, but this effect did not last up to 6 weeks. Histological analysis showed that Mg implantation promoted more angiogenesis in the second week after surgery, and gas bubbles caused by Mg degradation were observed in the sockets (**Figure 8**).

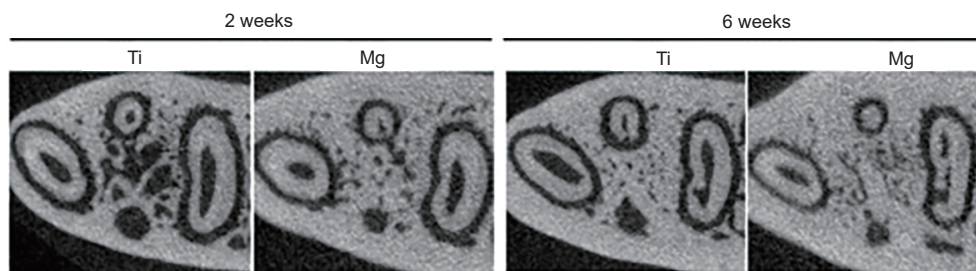


**Figure 8.** Mg rod for mandibular repair in rats. Mg: magnesium; Ti: titanium. Reprinted from He et al.<sup>123</sup> Copyright 2020, with permission from American Academy of Periodontology.

In order to investigate the biodegradability of Mg-calcium (Ca)-strontium (Sr) alloy and its effects on surrounding tissues, Berglund et al.<sup>124</sup> implanted Mg-1.0wt.% Ca-0.5wt.% Sr alloy pins into the tibiae of rats. All rats tolerated the implant well and only mild swelling was observed within 4 days after surgery. No signs of infection were found. According to three-dimensional reconstructions, the implant was almost completely decomposed by 6 weeks after surgery, retaining only 10% of its original volume. As the implant degraded, it continued to be replaced by new bone, and excellent bone

repair was achieved at 6 weeks postoperatively. According to the histological results, gas from implant degradation was observed at 1 and 3 weeks and the voids disappeared at 6 weeks, possibly because the gas had been absorbed. Although there was local gas accumulation, no microfractures were seen in the bone. Quantification of the number of osteoclasts showed that the number reached a peak at 3 weeks but had decreased significantly at 6 weeks, demonstrating that the implant was well tolerated by the surrounding tissues (**Figure 9**).

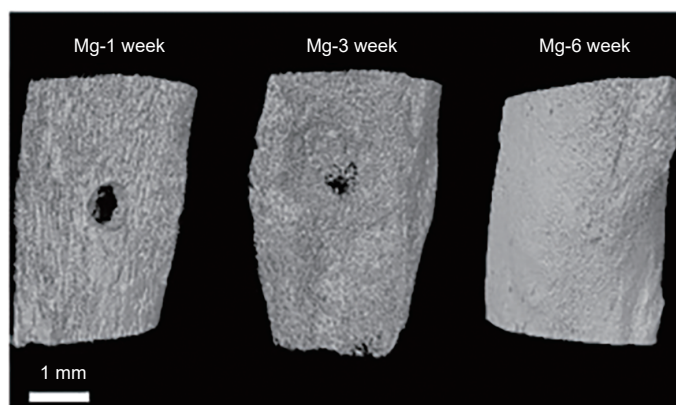


**Figure 9.** Bone morphology around magnesium (Mg) alloy implants at different time points. Scale bar: 1 mm. Reprinted from Berglund et al.<sup>124</sup>

#### Mouse model studies

Mg alloy containing 2% silver (Mg2Ag), which was cast and treated by a cooling process, has satisfactory mechanical properties and degradation rate and has demonstrated good biocompatibility *in vitro*.<sup>125</sup> To investigate the *in vivo* degradation and fracture healing of Mg2Ag, Jähn et al.<sup>126</sup> implanted Mg2Ag intramedullary nails into mice with and without femoral shaft fractures. The intramedullary nail showed a faster rate of degradation *in vivo* than *in vitro*, but no health abnormalities due to degradation were observed. The authors found that the Mg2Ag alloy inhibited osteoclast function *in vitro*, similarly to its effect *in vivo*, while implantation of the Mg2Ag intramedullary nail improved bone formation during bone remodelling and reduced bone resorption.

Yoshizawa et al.<sup>127</sup> constructed a stem cell implantation model in immunocompromised mice in order to investigate the long-term biological role of Mg alloy *in vivo* and its effect on human bone marrow stromal cells. The authors inserted pure Mg or Mg alloy AZ31 into collagen sponge scaffolds seeded

with human bone marrow stromal cells and implanted the scaffolds subcutaneously in mice. Eight weeks after surgery, the degradation and biological effects of the implants were investigated. The results showed that pure magnesium degraded faster than AZ31, but both had good biocompatibility. Immunohistochemistry showed that matrix protein 1 and osteopontin were expressed around the implants, and the authors found a thin mineral layer around the implants.

#### Rabbit model studies

Han et al.<sup>128</sup> fabricated a bone screw for fixation of bone fractures in the distal femur of rabbits. The screws were created using Hp Mg materials that went through a rolling process in advance. Because of the mechanical stress at the implant site, the corrosion rate of the screw at 4 weeks post-operation was higher than that after 4 weeks immersion, and the corrosion rate showed a significant linear correlation with time up to 24 weeks post-operation. Hp Mg screws showed ideal degradation performance throughout the experiment.

Compared with a poly-L-lactic acid group, the Hp MG group had better osteogenic performance, and irregular woven bone was observed in the fourth week without any apparent biosafety problems (Figure 10).

Hung et al.<sup>129</sup> investigated the bone marrow space in fractured rabbit ulnae fixated using Mg-based plates and screws. Micro-CT analysis of rabbit ulna samples showed the presence of radiopaque mineralised tissues in the medullary cavity at 8

weeks postoperatively, while intensive bone remodelling and more mineralised deposition were found at 16 weeks after surgery. Based on the result *in vitro*, the authors suggest that the osteogenic effect of Mg is mediated by activating the canonical Wnt signalling pathway (Figure 11). In addition, Mg-based interference screws are considered to have satisfactory repair capabilities in the rabbit anterior cruciate ligament reconstruction model.<sup>130</sup>



**Figure 10.** Magnesium screws for repair of distal femoral fractures in rabbits. Reprinted from Han et al.<sup>128</sup> Copyright 2015, with permission from Elsevier.

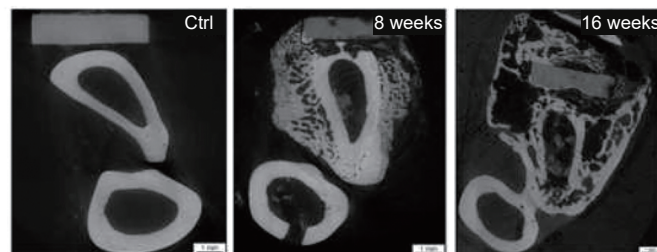


**Figure 11.** Magnesium-based plates and screws for the treatment of ulnar fractures in rabbits. Scale bars: 1 mm. Reprinted from Hung et al.<sup>129</sup> Copyright 2019, with permission from Elsevier Ltd. on behalf of Acta Materialia Inc.

Li et al.<sup>131</sup> studied the therapeutic effect of Mg-copper (Cu) alloy on osteomyelitis in rabbits. The alloys are made of high purity Mg and pure Cu powder, and designated Mg0Cu, Mg0.05Cu, Mg0.1Cu and Mg0.25Cu according to the content proportion of Cu in the alloy. Mg0.25Cu alloy has an obvious antibacterial effect *in vitro*. The authors constructed a rabbit model of chronic osteomyelitis in the tibia which was induced by methicillin-resistant *S. aureus* and then implanted the Mg0.25Cu alloy into the model. Haematoxylin and eosin staining of the heart, liver, spleen, lung, and kidney, blood biochemical tests and the stable body temperatures and weights of the animals demonstrated the good biocompatibility of the alloy. Histological evaluation at 4 weeks postoperatively demonstrated that Mg0.25Cu nails inhibited bone infection, with only a slight inflammatory response around the implant and almost no inflammatory cells in the tibial marrow cavity. Digital X-ray and magnetic resonance images revealed that the Mg0.25Cu nails were partially degraded, small amounts of gas were released and a slight periosteal reaction was induced. The bone defect caused by infection was repaired and regeneration

of thin cortical bone was observed.

The alloy thus appears effective in controlling the corrosion rate of Mg-based implants when applied as a coating on the surface of the implants.

Jiang et al.<sup>132</sup> prepared a novel coating on the surface of AZ31 Mg alloy through poly dopamine (PDA)-mediated assembly of hydroxyapatite (HA) nanoparticles and added the growth factor bone morphogenetic protein-2 (BMP-2); the materials were named PDA@HA and PDA@HA&BMP-2 according to whether or not they contained BMP-2. The coating improved the biocompatibility and corrosion rate of the Mg-based implants and provided sustained release of BMP-2 *in vitro*. A rabbit critical-sized femoral defect model was constructed and implanted with PDA@HA-coated AZ31 and PDA@HA&BMP-2-coated AZ31. During the experiment, the rabbits showed no abnormal behaviour or instances of wound infection. The implants were removed 12 weeks after surgery and gross observation showed that they were still firmly attached to the femur. Histological analysis showed

that no polymorphonuclear cells were present in any of the groups, suggesting that the coating and the exposed AZ31 after degradation of the coating did not cause adverse effects on surrounding tissues. Better bone repair was observed in the PDA@HA&BMP-2 group compared to the PDA@HA

group and small empty cavities were observed around the new bone and implants, possibly due to hydrogen generated during the degradation process. The cavities in the PDA@HA&BMP-2 group were smaller than those in the other groups (**Figure 12**).

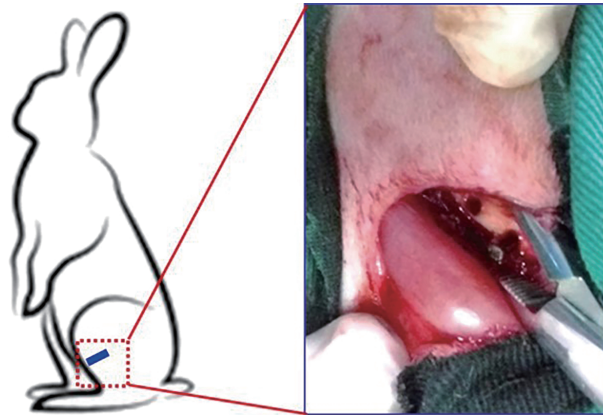


**Figure 12.** Schematic diagram showing the surgical process in the rabbit femoral defect model. Reprinted from Jiang et al.<sup>132</sup> Copyright 2017 Wiley Periodicals, Inc. Reproduced with permission.

#### Other animal model studies

Absorbable implants that can avoid the need for a secondary surgery are of great importance in paediatric orthopaedics. However, due to differences in bone metabolism between adults and children, it is not sufficient to validate biodegradable implants only in adult animal models. Grün et al.<sup>133</sup> developed a lean Mg–Zn–Ca alloy (MgZnCa; < 0.5 wt% Zn and < 0.5 wt% Ca; ZX00) for children and investigated its degradation and bone formation properties in a small rodent and a large ovine

model. The alloy was implanted into the femur of Sprague-Dawley rats and the right proximal tibiae of 1-month-old female lambs. After surgery, gas release occurred in both large and small animal models, but did not affect bone formation, although gas release accelerated at 12 weeks in rats and 6 weeks in the ovine model. There was no significant difference in implant degradation rate between the two models, and osseointegration was observed according to micro-CT and histological results in both models (**Figure 13**).

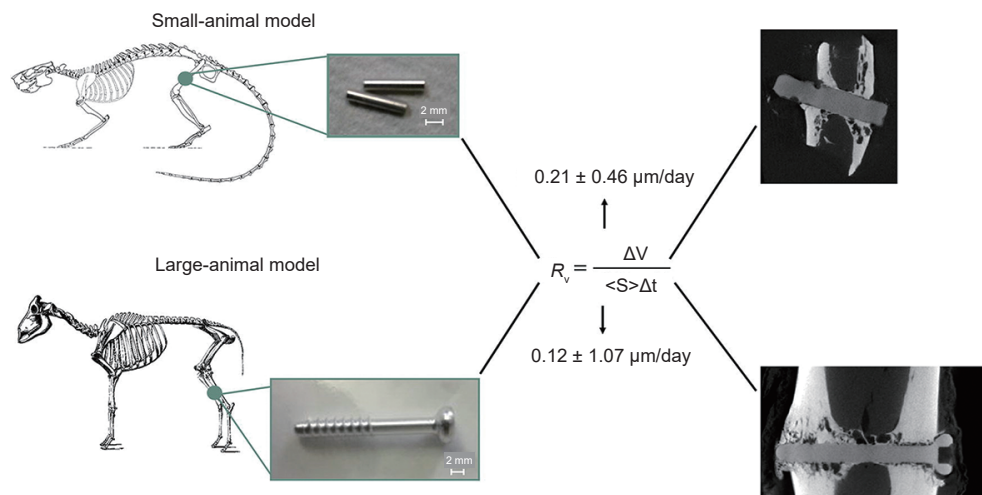


**Figure 13.** The use of magnesium alloy implants in large and small animal models. Scale bars: 2 mm. Reprinted with permission from Grün et al.<sup>133</sup> Copyright 2018, Acta Materialia Inc.

Marukawa et al.<sup>134</sup> assessed anodised WE43 (containing Mg, yttrium, rare earth elements and zirconium; Elektron SynerMag<sup>®</sup>) Mg alloy, monolithic WE43 Mg alloy and poly-L-lactic acid in 1-year-old beagle dogs. Bone osteotomy was performed in the tibiae of the dogs, then screws fabricated from the test materials were used to fix the osteotomy. At 4 and 12 weeks after surgery, loosening and breakage in the

anodised WE43 group and the monolithic WE43 group were both better than in the poly-L-lactic acid group. At 4 weeks postoperatively, bone resorption and gas formation were observed around the monolithic WE43 implants, while in the anodised WE43 group, no bone resorption was observed, gas production was less and new bone formation was better. At 12 weeks postoperatively, bone maturation had progressed in

all groups, but gas cavities remained in the monolithic WE43 group.

The miniature pig is a useful large-animal model for dental and orofacial research. The advantage of this model is that the size of the plates/screws available and the soft tissue properties in the midface and the skull bone are similar to those of humans.<sup>135</sup> Schaller et al.<sup>17</sup> used the Mg alloy WE43 as an implant which was tested in the frontal bone of adult miniature pigs. Half of the Mg implants received a plasma electrolytic coating. No complications due to the implant were observed during the experiment. Subcutaneous gas pocket formation of uncoated Mg implants due to implant degradation was observed one week after surgery. This did not occur in the coated Mg implant group. At 12 and 24 weeks after surgery, no complete corrosion was observed in any of the implants, and the implanted group had better bone formation than the uncoated implant group. Histological analysis showed that no inflammatory cells or increases in the number of osteoclasts were observed around the implants.

### Animal models for research into the use of magnesium-based materials in other tissues

Metal stents can be used for the treatment of cardiovascular diseases, such as arterial stenoses, but long-term implantation of nondegradable metal implants may induce a restenosis-like reaction and impair tissue function.<sup>136</sup> The use of biodegradable implants to avoid this problem is a promising option. Mg-based implants are attracting attention as a new biodegradable metal implant in the treatment of cardiovascular diseases.<sup>137-139</sup> Bowen et al.<sup>140</sup> implanted pure Mg wires in the abdominal aortae of rats to investigate degradation correlations *in vivo* and *in vitro*. The results showed that the *in vitro* penetration rate was higher than the *in vivo* degradation rate by a factor of 1.2–1.9× (±0.2×). Waksman et al.<sup>141</sup> deployed Mg alloy stents in coronary arteries of pigs, and found that the Mg alloy caused no obvious discomfort in the pigs and was associated with less neointima formation. Mg alloy vascular implants have been extensively studied, but the control of their high reactivity and degradability in physiological environment is still a concern.<sup>142-145</sup>

### Summary and Outlook

A lot of research has been carried out on animal models that are used in bone tissue engineering, and the use of small rodents accounts for more than half of them.<sup>146, 147</sup> Because of their low cost and clear genetic background, rodent models are often used for basic research questions, and translational research often uses large animal models to simulate the biomechanical requirements of human patients.<sup>148</sup> For translational research, the devices and materials should also be as close to clinical specifications as possible, such as nails, plates, and retainers.<sup>149</sup> In order to maximise the translational potential of such studies, it is necessary to carefully select appropriate age, sex, animal species, and clinically-relevant outcome indicators, and ensure that there is sufficient statistical capacity to address research questions.

As a new generation of bone implant materials, Mg-based materials have received extensive attention due to their

excellent biocompatibility, degradability and osteogenic activity. Currently, various strategies have been developed to improve the degradation and mechanical properties of Mg-based implants, include alloying and surface Mg; these methods may broaden the use of Mg-based materials.<sup>2</sup> Numerous studies conducted on the effects of Mg-based materials *in vivo* have demonstrated a beneficial effect on bone tissue repair, and these encouraging results show the revolutionary promise of Mg-based materials in the treatment of refractory bone diseases, including osteoporotic fractures and osteomyelitis. According to published reports, Mg-based materials have been successfully used in patients with non-load-bearing site fractures, which shows the broad clinical application prospect of Mg-based materials.<sup>2, 150</sup> Based on a full understanding of the physical, chemical and biological properties of Mg and its alloys, the wider use of Mg-based materials in the clinic will be possible.

### Author contributions

XJ, TS, XG designed the review; XJ defined the intellectual content; XJ, QD, WS and KY performed the literature searches; XJ, QD, WS, KY, YS, BY, QW, QG, TS acquired the data; XJ, QD, WS and KY performed the data analysis; XJ prepared and finished the manuscript; XJ, QD, WS and KY edited the manuscript; XJ, QD, WS, KY and YS reviewed the manuscript; XG supervised manuscript drafting and determined the final draft. All authors reviewed and approved the final version of the manuscript.

### Financial support

This work was supported by the National Key R&D Program of China (No. 2016YFC1100100), the National Natural Science Foundation of China (Nos. 81672158, 81873999) and the Youth Program of the National Natural Science Foundation of China (No. 81902219).

### Acknowledgement

We thank Prof. Qian Wang from the University of South Carolina, and Prof. Zengwu Shao from Wuhan Union Hospital, for their considerate suggestions.

### Conflicts of interest statement

The authors declare no conflict of interest.

Editor note: Xiaodong Guo is an Editorial Board member of *Biomaterials Translational*. He was blinded from reviewing or making decisions on the manuscript. The article was subject to the journal's standard procedures, with peer review handled independently of this Editorial Board member and his research group.

### Open access statement

This is an open access journal, and articles are distributed under the terms of the Creative Commons Attribution-NonCommercial-ShareAlike 4.0 License, which allows others to remix, tweak, and build upon the work non-commercially, as long as appropriate credit is given and the new creations are licensed under the identical terms.

1. Karinkanta, S.; Piirtola, M.; Sievänen, H.; Uusi-Rasi, K.; Kannus, P. Physical therapy approaches to reduce fall and fracture risk among older adults. *Nat Rev Endocrinol.* **2010**, *6*, 396-407.
2. Zhao, D.; Witte, F.; Lu, F.; Wang, J.; Li, J.; Qin, L. Current status on clinical applications of magnesium-based orthopaedic implants: A review from clinical translational perspective. *Biomaterials.* **2017**, *112*, 287-302.
3. Sha, M.; Guo, Z.; Fu, J.; Li, J.; Yuan, C. F.; Shi, L.; Li, S. J. The effects of nail rigidity on fracture healing in rats with osteoporosis. *Acta Orthop.* **2009**, *80*, 135-138.
4. Singhvi, M. S.; Zinjarde, S. S.; Gokhale, D. V. Polylactic acid: synthesis and biomedical applications. *J Appl Microbiol.* **2019**, *127*, 1612-1626.
5. Zhao, D.; Zhu, T.; Li, J.; Cui, L.; Zhang, Z.; Zhuang, X.; Ding, J. Poly(lactic-co-glycolic acid)-based composite bone-substitute materials.

- Bioact Mater.* **2021**, *6*, 346-360.
6. Wang, J. L.; Xu, J. K.; Hopkins, C.; Chow, D. H.; Qin, L. Biodegradable magnesium-based implants in orthopedics—a general review and perspectives. *Adv Sci (Weinh)*. **2020**, *7*, 1902443.
  7. Navarro, M.; Michiardi, A.; Castaño, O.; Planell, J. A. Biomaterials in orthopaedics. *J R Soc Interface*. **2008**, *5*, 1137-1158.
  8. Barber, F. A.; Dockery, W. D. Long-term absorption of poly-L-lactic Acid interference screws. *Arthroscopy*. **2006**, *22*, 820-826.
  9. Cheung, W. H.; Miclau, T.; Chow, S. K.; Yang, F. F.; Alt, V. Fracture healing in osteoporotic bone. *Injury*. **2016**, *47* Suppl 2, S21-26.
  10. Zheng, N.; Tang, N.; Qin, L. Atypical femoral fractures and current management. *J Orthop Translat*. **2016**, *7*, 7-22.
  11. Farraro, K. F.; Sasaki, N.; Woo, S. L.; Kim, K. E.; Tei, M. M.; Speziali, A.; McMahon, P. J. Magnesium ring device to restore function of a transected anterior cruciate ligament in the goat stifle joint. *J Orthop Res*. **2016**, *34*, 2001-2008.
  12. Xia, J.; Chen, H.; Yan, J.; Wu, H.; Wang, H.; Guo, J.; Zhang, X.; Zhang, S.; Zhao, C.; Chen, Y. High-purity magnesium staples suppress inflammatory response in rectal anastomoses. *ACS Appl Mater Interfaces*. **2017**, *9*, 9506-9515.
  13. Naujokat, H.; Ruff, C. B.; Klüter, T.; Seitz, J. M.; Açil, Y.; Wiltfang, J. Influence of surface modifications on the degradation of standard-sized magnesium plates and healing of mandibular osteotomies in miniature pigs. *Int J Oral Maxillofac Surg*. **2020**, *49*, 272-283.
  14. Krämer, M.; Schilling, M.; Eifler, R.; Hering, B.; Reifenrath, J.; Besdo, S.; Windhagen, H.; Willbold, E.; Weizbauer, A. Corrosion behavior, biocompatibility and biomechanical stability of a prototype magnesium-based biodegradable intramedullary nailing system. *Mater Sci Eng C Mater Biol Appl*. **2016**, *59*, 129-135.
  15. Erbel, R.; Di Mario, C.; Bartunek, J.; Bonnier, J.; de Bruyne, B.; Eberli, F. R.; Erne, P.; Haude, M.; Heublein, B.; Horrigan, M.; Illesley, C.; Böse, D.; Koolen, J.; Lüscher, T. F.; Weissman, N.; Waksman, R.; Temporary scaffolding of coronary arteries with bioabsorbable magnesium stents: a prospective, n.-r. m. t. Temporary scaffolding of coronary arteries with bioabsorbable magnesium stents: a prospective, non-randomised multicentre trial. *Lancet*. **2007**, *369*, 1869-1875.
  16. Wu, J.; Lee, B.; Saha, P.; P, N. K. A feasibility study of biodegradable magnesium-aluminum-zinc-calcium-manganese (AZXM) alloys for tracheal stent application. *J Biomater Appl*. **2019**, *33*, 1080-1093.
  17. Schaller, B.; Saulacic, N.; Imwinkelried, T.; Beck, S.; Liu, E. W.; Gralla, J.; Nakahara, K.; Hofstetter, W.; Iizuka, T. In vivo degradation of magnesium plate/screw osteosynthesis implant systems: Soft and hard tissue response in a calvarial model in miniature pigs. *J Craniomaxillofac Surg*. **2016**, *44*, 309-317.
  18. Guo, X.; Xu, H.; Zhang, F.; Lu, F. Bioabsorbable high-purity magnesium interbody cage: degradation, interbody fusion, and biocompatibility from a goat cervical spine model. *Ann Transl Med*. **2020**, *8*, 1054.
  19. Zhao, Y.; Yu, S.; Wu, X.; Dai, H.; Liu, W.; Tu, R.; Goto, T. Construction of macroporous magnesium phosphate-based bone cement with sustained drug release. *Mater Des*. **2021**, *200*, 109466.
  20. Lai, Y.; Li, Y.; Cao, H.; Long, J.; Wang, X.; Li, L.; Li, C.; Jia, Q.; Teng, B.; Tang, T.; Peng, J.; Eglin, D.; Alini, M.; Grijpma, D. W.; Richards, G.; Qin, L. Osteogenic magnesium incorporated into PLGA/TCP porous scaffold by 3D printing for repairing challenging bone defect. *Biomaterials*. **2019**, *197*, 207-219.
  21. Zhang, D.; Ni, N.; Su, Y.; Miao, H.; Tang, Z.; Ji, Y.; Wang, Y.; Gao, H.; Ju, Y.; Sun, N.; Sun, H.; Yuan, G.; Wang, Y.; Zhou, H.; Huang, H.; Gu, P.; Fan, X. Targeting local osteogenic and ancillary cells by mechanobiologically optimized magnesium scaffolds for orbital bone reconstruction in canines. *ACS Appl Mater Interfaces*. **2020**, *12*, 27889-27904.
  22. Chakraborty Banerjee, P.; Al-Saadi, S.; Choudhary, L.; Harandi, S. E.; Singh, R. Magnesium implants: prospects and challenges. *Materials (Basel)*. **2019**, *12*, 136.
  23. Agarwal, S.; Curtin, J.; Duffy, B.; Jaiswal, S. Biodegradable magnesium alloys for orthopaedic applications: A review on corrosion, biocompatibility and surface modifications. *Mater Sci Eng C Mater Biol Appl*. **2016**, *68*, 948-963.
  24. Zhao, D.; Huang, S.; Lu, F.; Wang, B.; Yang, L.; Qin, L.; Yang, K.; Li, Y.; Li, W.; Wang, W.; Tian, S.; Zhang, X.; Gao, W.; Wang, Z.; Zhang, Y.; Xie, X.; Wang, J.; Li, J. Vascularized bone grafting fixed by biodegradable magnesium screw for treating osteonecrosis of the femoral head. *Biomaterials*. **2016**, *81*, 84-92.
  25. Witte, F.; Kaese, V.; Haferkamp, H.; Switzer, E.; Meyer-Lindenberg, A.; Wirth, C. J.; Windhagen, H. In vivo corrosion of four magnesium alloys and the associated bone response. *Biomaterials*. **2005**, *26*, 3557-3563.
  26. Zhang, J.; Shang, Z.; Jiang, Y.; Zhang, K.; Li, X.; Ma, M.; Li, Y.; Ma, B. Biodegradable metals for bone fracture repair in animal models: a systematic review. *Regen Biomater*. **2021**, *8*, rbaa047.
  27. Seitz, J. M.; Eifler, R.; Bach, F. W.; Maier, H. J. Magnesium degradation products: effects on tissue and human metabolism. *J Biomed Mater Res A*. **2014**, *102*, 3744-3753.
  28. Gonzalez, J.; Hou, R. Q.; Nidadavolu, E. P. S.; Willumeit-Römer, R.; Feyerabend, F. Magnesium degradation under physiological conditions - Best practice. *Bioact Mater*. **2018**, *3*, 174-185.
  29. Walker, J.; Shadanbaz, S.; Woodfield, T. B.; Staiger, M. P.; Dias, G. J. Magnesium biomaterials for orthopedic application: a review from a biological perspective. *J Biomed Mater Res B Appl Biomater*. **2014**, *102*, 1316-1331.
  30. Oshibe, N.; Marukawa, E.; Yoda, T.; Harada, H. Degradation and interaction with bone of magnesium alloy WE43 implants: A long-term follow-up in vivo rat tibia study. *J Biomater Appl*. **2019**, *33*, 1157-1167.
  31. Holweg, P.; Berger, L.; Cihova, M.; Donohue, N.; Clement, B.; Schwarze, U.; Sommer, N. G.; Hohenberger, G.; van den Beucken, J.; Seibert, F.; Leithner, A.; Löffler, J. F.; Weinberg, A. M. A lean magnesium-zinc-calcium alloy ZX00 used for bone fracture stabilization in a large growing-animal model. *Acta Biomater*. **2020**, *113*, 646-659.
  32. Han, H. S.; Jun, I.; Seok, H. K.; Lee, K. S.; Lee, K.; Witte, F.; Mantovani, D.; Kim, Y. C.; Glyn-Jones, S.; Edwards, J. R. Biodegradable magnesium alloys promote angio-osteogenesis to enhance bone repair. *Adv Sci (Weinh)*. **2020**, *7*, 2000800.
  33. Gao, J.; Su, Y.; Qin, Y. X. Calcium phosphate coatings enhance biocompatibility and degradation resistance of magnesium alloy: Correlating in vitro and in vivo studies. *Bioact Mater*. **2021**, *6*, 1223-1229.
  34. Liu, W.; Li, T.; Yang, C.; Wang, D.; He, G.; Cheng, M.; Wang, Q.; Zhang, X. Lithium-incorporated nanoporous coating formed by micro arc oxidation (MAO) on magnesium alloy with improved corrosion resistance, angiogenesis and osseointegration. *J Biomed Nanotechnol*. **2019**, *15*, 1172-1184.
  35. Helmholtz, H.; Will, O.; Penate-Medina, T.; Humbert, J.; Damm, T.; Luthringer-Feyerabend, B.; Willumeit-Römer, R.; Glüer, C. C.; Penate-Medina, O. Tissue responses after implantation of biodegradable Mg

- alloys evaluated by multimodality 3D micro-bioimaging in vivo. *J Biomed Mater Res A*. **2021**, *109*, 1521-1529.
36. Grada, A.; Mervis, J.; Falanga, V. Research techniques made simple: animal models of wound healing. *J Invest Dermatol*. **2018**, *138*, 2095-2105. e1.
  37. Ribitsch, I.; Baptista, P. M.; Lange-Consiglio, A.; Melotti, L.; Patrino, M.; Jenner, F.; Schnabl-Feichter, E.; Dutton, L. C.; Connolly, D. J.; van Steenbeek, F. G.; Dudhia, J.; Penning, L. C. Large animal models in regenerative medicine and tissue engineering: to do or not to do. *Front Bioeng Biotechnol*. **2020**, *8*, 972.
  38. Al Alawi, A. M.; Majoni, S. W.; Falhammar, H. Magnesium and human health: perspectives and research directions. *Int J Endocrinol*. **2018**, *2018*, 9041694.
  39. Romani, A. M. Cellular magnesium homeostasis. *Arch Biochem Biophys*. **2011**, *512*, 1-23.
  40. Wolf, F. I.; Trapani, V. Cell (patho)physiology of magnesium. *Clin Sci (Lond)*. **2008**, *114*, 27-35.
  41. de Baaij, J. H.; Hoenderop, J. G.; Bindels, R. J. Magnesium in man: implications for health and disease. *Physiol Rev*. **2015**, *95*, 1-46.
  42. Jahnen-Dechent, W.; Ketteler, M. Magnesium basics. *Clin Kidney J*. **2012**, *5*, i3-i14.
  43. Elin, R. J. Assessment of magnesium status for diagnosis and therapy. *Magnes Res*. **2010**, *23*, S194-198.
  44. Razzaque, M. S. Magnesium: are we consuming enough? *Nutrients*. **2018**, *10*, 1863.
  45. Yamanaka, R.; Shindo, Y.; Oka, K. Magnesium is a key player in neuronal maturation and neuropathology. *Int J Mol Sci*. **2019**, *20*, 3439.
  46. Yoshizawa, S.; Brown, A.; Barchowsky, A.; Sfeir, C. Magnesium ion stimulation of bone marrow stromal cells enhances osteogenic activity, simulating the effect of magnesium alloy degradation. *Acta Biomater*. **2014**, *10*, 2834-2842.
  47. Belluci, M. M.; de Molon, R. S.; Rossa, C., Jr.; Tetradis, S.; Giro, G.; Cerri, P. S.; Marcantonio, E., Jr.; Orrico, S. R. P. Severe magnesium deficiency compromises systemic bone mineral density and aggravates inflammatory bone resorption. *J Nutr Biochem*. **2020**, *77*, 108301.
  48. Ciosek, Z.; Kot, K.; Kosik-Bogacka, D.; Łanocha-Arendarczyk, N.; Rotter, I. The effects of calcium, magnesium, phosphorus, fluoride, and lead on bone tissue. *Biomolecules*. **2021**, *11*, 506.
  49. Zhai, Z.; Qu, X.; Li, H.; Yang, K.; Wan, P.; Tan, L.; Ouyang, Z.; Liu, X.; Tian, B.; Xiao, F.; Wang, W.; Jiang, C.; Tang, T.; Fan, Q.; Qin, A.; Dai, K. The effect of metallic magnesium degradation products on osteoclast-induced osteolysis and attenuation of NF- $\kappa$ B and NFATc1 signaling. *Biomaterials*. **2014**, *35*, 6299-6310.
  50. Xie, H.; Cui, Z.; Wang, L.; Xia, Z.; Hu, Y.; Xian, L.; Li, C.; Xie, L.; Crane, J.; Wan, M.; Zhen, G.; Bian, Q.; Yu, B.; Chang, W.; Qiu, T.; Pickarski, M.; Duong, L. T.; Windle, J. J.; Luo, X.; Liao, E.; Cao, X. PDGF-BB secreted by preosteoclasts induces angiogenesis during coupling with osteogenesis. *Nat Med*. **2014**, *20*, 1270-1278.
  51. Maier, J. A.; Castiglioni, S.; Locatelli, L.; Zocchi, M.; Mazur, A. Magnesium and inflammation: advances and perspectives. *Semin Cell Dev Biol*. **2021**, *115*, 37-44.
  52. Zheng, Z.; Chen, Y.; Hong, H.; Shen, Y.; Wang, Y.; Sun, J.; Wang, X. The "Yin and Yang" of immunomodulatory magnesium-enriched graphene oxide nanoscrolls decorated biomimetic scaffolds in promoting bone regeneration. *Adv Healthc Mater*. **2021**, *10*, e2000631.
  53. Chen, Z.; Mao, X.; Tan, L.; Friis, T.; Wu, C.; Crawford, R.; Xiao, Y. Osteoimmunomodulatory properties of magnesium scaffolds coated with  $\beta$ -tricalcium phosphate. *Biomaterials*. **2014**, *35*, 8553-8565.
  54. Libako, P.; Nowacki, W.; Castiglioni, S.; Mazur, A.; Maier, J. A. Extracellular magnesium and calcium blockers modulate macrophage activity. *Magnes Res*. **2016**, *29*, 11-21.
  55. Li, Z.; Meyers, C. A.; Chang, L.; Lee, S.; Li, Z.; Tomlinson, R.; Hoke, A.; Clemens, T. L.; James, A. W. Fracture repair requires TrkA signaling by skeletal sensory nerves. *J Clin Invest*. **2019**, *129*, 5137-5150.
  56. Zhang, Y.; Xu, J.; Ruan, Y. C.; Yu, M. K.; O'Laughlin, M.; Wise, H.; Chen, D.; Tian, L.; Shi, D.; Wang, J.; Chen, S.; Feng, J. Q.; Chow, D. H.; Xie, X.; Zheng, L.; Huang, L.; Huang, S.; Leung, K.; Lu, N.; Zhao, L.; Li, H.; Zhao, D.; Guo, X.; Chan, K.; Witte, F.; Chan, H. C.; Zheng, Y.; Qin, L. Implant-derived magnesium induces local neuronal production of CGRP to improve bone-fracture healing in rats. *Nat Med*. **2016**, *22*, 1160-1169.
  57. Michailova, A. P.; Belik, M. E.; McCulloch, A. D. Effects of magnesium on cardiac excitation-contraction coupling. *J Am Coll Nutr*. **2004**, *23*, 514s-517s.
  58. Teragawa, H.; Matsuura, H.; Chayama, K.; Oshima, T. Mechanisms responsible for vasodilation upon magnesium infusion in vivo: clinical evidence. *Magnes Res*. **2002**, *15*, 241-246.
  59. Teragawa, H.; Kato, M.; Yamagata, T.; Matsuura, H.; Kajiyama, G. Magnesium causes nitric oxide independent coronary artery vasodilation in humans. *Heart*. **2001**, *86*, 212-216.
  60. Cochrane, D. E.; Douglas, W. W. Histamine release by exocytosis from rat mast cells on reduction of extracellular sodium: a secretory response inhibited by calcium, strontium, barium or magnesium. *J Physiol*. **1976**, *257*, 433-448.
  61. Komaki, F.; Akiyama, T.; Yamazaki, T.; Kitagawa, H.; Nosaka, S.; Shirai, M. Effects of intravenous magnesium infusion on in vivo release of acetylcholine and catecholamine in rat adrenal medulla. *Auton Neurosci*. **2013**, *177*, 123-128.
  62. Hashimoto, Y.; Nishimura, Y.; Maeda, H.; Yokoyama, M. Assessment of magnesium status in patients with bronchial asthma. *J Asthma*. **2000**, *37*, 489-496.
  63. Amin, M.; Abdel-Fattah, M.; Zaghoul, S. S. Magnesium concentration in acute asthmatic children. *Iran J Pediatr*. **2012**, *22*, 463-467.
  64. Hashim Ali Hussein, S.; Nielsen, L. P.; Konow Bøgebjerg Dolberg, M.; Dahl, R. Serum magnesium and not vitamin D is associated with better QoL in COPD: A cross-sectional study. *Respir Med*. **2015**, *109*, 727-733.
  65. Gumus, A.; Haziroglu, M.; Gunes, Y. Association of serum magnesium levels with frequency of acute exacerbations in chronic obstructive pulmonary disease: a prospective study. *Pulm Med*. **2014**, *2014*, 329476.
  66. Niinomi, M. Metallic biomaterials. *J Artif Organs*. **2008**, *11*, 105-110.
  67. Niinomi, M.; Nakai, M.; Hieda, J. Development of new metallic alloys for biomedical applications. *Acta Biomater*. **2012**, *8*, 3888-3903.
  68. Chen, J.; Tan, L.; Yu, X.; Etim, I. P.; Ibrahim, M.; Yang, K. Mechanical properties of magnesium alloys for medical application: a review. *J Mech Behav Biomed Mater*. **2018**, *87*, 68-79.
  69. Staiger, M. P.; Pietak, A. M.; Huadmai, J.; Dias, G. Magnesium and its alloys as orthopedic biomaterials: a review. *Biomaterials*. **2006**, *27*, 1728-1734.
  70. Liu, C.; Ren, Z.; Xu, Y.; Pang, S.; Zhao, X.; Zhao, Y. Biodegradable magnesium alloys developed as bone repair materials: a review. *Scanning*. **2018**, *2018*, 9216314.
  71. Ding, W. Opportunities and challenges for the biodegradable magnesium alloys as next-generation biomaterials. *Regen Biomater*. **2016**, *3*, 79-86.
  72. Kirkland, N. T.; Birbilis, N.; Staiger, M. P. Assessing the corrosion of biodegradable magnesium implants: a critical review of current

- methodologies and their limitations. *Acta Biomater.* **2012**, *8*, 925-936.
73. Kawasaki, H.; Guan, J.; Tamama, K. Hydrogen gas treatment prolongs replicative lifespan of bone marrow multipotential stromal cells in vitro while preserving differentiation and paracrine potentials. *Biochem Biophys Res Commun.* **2010**, *397*, 608-613.
  74. Kamrani, S.; Fleck, C. Biodegradable magnesium alloys as temporary orthopaedic implants: a review. *Biomaterials.* **2019**, *32*, 185-193.
  75. Jang, Y.; Collins, B.; Sankar, J.; Yun, Y. Effect of biologically relevant ions on the corrosion products formed on alloy AZ31B: an improved understanding of magnesium corrosion. *Acta Biomater.* **2013**, *9*, 8761-8770.
  76. Wagener, V.; Faltz, A. S.; Killian, M. S.; Schmuki, P.; Virtanen, S. Protein interactions with corroding metal surfaces: comparison of Mg and Fe. *Faraday Discuss.* **2015**, *180*, 347-360.
  77. Bobby Kannan, M.; Singh Raman, R. K.; Witte, F.; Blawert, C.; Dietzel, W. Influence of circumferential notch and fatigue crack on the mechanical integrity of biodegradable magnesium-based alloy in simulated body fluid. *J Biomed Mater Res B Appl Biomater.* **2011**, *96*, 303-309.
  78. Kuhlmann, J.; Bartsch, I.; Willbold, E.; Schuchardt, S.; Holz, O.; Hort, N.; Höche, D.; Heineman, W. R.; Witte, F. Fast escape of hydrogen from gas cavities around corroding magnesium implants. *Acta Biomater.* **2013**, *9*, 8714-8721.
  79. Yang, J.; Koons, G. L.; Cheng, G.; Zhao, L.; Mikos, A. G.; Cui, F. A review on the exploitation of biodegradable magnesium-based composites for medical applications. *Biomed Mater.* **2018**, *13*, 022001.
  80. Taguchi, T.; Lopez, M. J. An overview of de novo bone generation in animal models. *J Orthop Res.* **2021**, *39*, 7-21.
  81. Bigham-Sadegh, A.; Oryan, A. Selection of animal models for pre-clinical strategies in evaluating the fracture healing, bone graft substitutes and bone tissue regeneration and engineering. *Connect Tissue Res.* **2015**, *56*, 175-194.
  82. Pfeiffenberger, M.; Damerau, A.; Lang, A.; Buttgerit, F.; Hoff, P.; Gaber, T. Fracture healing research-shift towards in vitro modeling? *Biomedicines.* **2021**, *9*, 748.
  83. Spicer, P. P.; Kretlow, J. D.; Young, S.; Jansen, J. A.; Kasper, F. K.; Mikos, A. G. Evaluation of bone regeneration using the rat critical size calvarial defect. *Nat Protoc.* **2012**, *7*, 1918-1929.
  84. Dubey, N.; Ferreira, J. A.; Malda, J.; Bhaduri, S. B.; Bottino, M. C. Extracellular matrix/amorphous magnesium phosphate bioink for 3D bioprinting of craniomaxillofacial bone tissue. *ACS Appl Mater Interfaces.* **2020**, *12*, 23752-23763.
  85. Yuan, Z.; Wei, P.; Huang, Y.; Zhang, W.; Chen, F.; Zhang, X.; Mao, J.; Chen, D.; Cai, Q.; Yang, X. Injectable PLGA microspheres with tunable magnesium ion release for promoting bone regeneration. *Acta Biomater.* **2019**, *85*, 294-309.
  86. Gomes, P. S.; Fernandes, M. H. Rodent models in bone-related research: the relevance of calvarial defects in the assessment of bone regeneration strategies. *Lab Anim.* **2011**, *45*, 14-24.
  87. Fang, B.; Qiu, P.; Xia, C.; Cai, D.; Zhao, C.; Chen, Y.; Wang, H.; Liu, S.; Cheng, H.; Tang, Z.; Wang, B.; Fan, S.; Lin, X. Extracellular matrix scaffold crosslinked with vancomycin for multifunctional antibacterial bone infection therapy. *Biomaterials.* **2021**, *268*, 120603.
  88. Dong, Y.; Liu, W.; Lei, Y.; Wu, T.; Zhang, S.; Guo, Y.; Liu, Y.; Chen, D.; Yuan, Q.; Wang, Y. Effect of gelatin sponge with colloid silver on bone healing in infected cranial defects. *Mater Sci Eng C Mater Biol Appl.* **2017**, *70*, 371-377.
  89. Reichert, J. C.; Saifzadeh, S.; Wullschlegel, M. E.; Epari, D. R.; Schütz, M. A.; Duda, G. N.; Schell, H.; van Griensven, M.; Redl, H.; Hutmacher, D. W. The challenge of establishing preclinical models for segmental bone defect research. *Biomaterials.* **2009**, *30*, 2149-2163.
  90. Gunderson, Z. J.; Campbell, Z. R.; McKinley, T. O.; Natoli, R. M.; Kacena, M. A. A comprehensive review of mouse diaphyseal femur fracture models. *Injury.* **2020**, *51*, 1439-1447.
  91. den Boer, F. C.; Patka, P.; Bakker, F. C.; Wippermann, B. W.; van Lingen, A.; Vink, G. Q.; Boshuizen, K.; Haarman, H. J. New segmental long bone defect model in sheep: quantitative analysis of healing with dual energy x-ray absorptiometry. *J Orthop Res.* **1999**, *17*, 654-660.
  92. Christou, C.; Oliver, R. A.; Pelletier, M. H.; Walsh, W. R. Ovine model for critical-size tibial segmental defects. *Comp Med.* **2014**, *64*, 377-385.
  93. Gugala, Z.; Lindsey, R. W.; Gogolewski, S. New Approaches in the treatment of critical-size segmental defects in long bones. *Macromol Symp.* **2007**, *253*, 147-161.
  94. McKinley, T. O.; Natoli, R. M.; Fischer, J. P.; Rytlewski, J. D.; Scofield, D. C.; Usmani, R.; Kuzma, A.; Griffin, K. S.; Jewell, E.; Childress, P.; Shively, K. D.; Chu, T. G.; Anglen, J. O.; Kacena, M. A. Internal fixation construct and defect size affect healing of a translational porcine diaphyseal tibial segmental bone defect. *Mil Med.* **2020**. doi: 10.1093/milmed/usaa516.
  95. Yavari, S. A.; van der Stok, J.; Ahmadi, S. M.; Wauthle, R.; Schrooten, J.; Weinans, H.; Zadpoor, A. A. Mechanical analysis of a rodent segmental bone defect model: the effects of internal fixation and implant stiffness on load transfer. *J Biomech.* **2014**, *47*, 2700-2708.
  96. Perren, S. M. Evolution of the internal fixation of long bone fractures. The scientific basis of biological internal fixation: choosing a new balance between stability and biology. *J Bone Joint Surg Br.* **2002**, *84*, 1093-1110.
  97. Bottagisio, M.; Coman, C.; Lovati, A. B. Animal models of orthopaedic infections. A review of rabbit models used to induce long bone bacterial infections. *J Med Microbiol.* **2019**, *68*, 506-537.
  98. Roux, K. M.; Cobb, L. H.; Seitz, M. A.; Priddy, L. B. Innovations in osteomyelitis research: A review of animal models. *Animal Model Exp Med.* **2021**, *4*, 59-70.
  99. Couly, G. F.; Coltey, P. M.; Le Douarin, N. M. The triple origin of skull in higher vertebrates: a study in quail-chick chimeras. *Development.* **1993**, *117*, 409-429.
  100. Reichert, J. C.; Gohlke, J.; Friis, T. E.; Quent, V. M.; Hutmacher, D. W. Mesodermal and neural crest derived ovine tibial and mandibular osteoblasts display distinct molecular differences. *Gene.* **2013**, *525*, 99-106.
  101. Liu, G.; Guo, Y.; Zhang, L.; Wang, X.; Liu, R.; Huang, P.; Xiao, Y.; Chen, Z.; Chen, Z. A standardized rat burr hole defect model to study maxillofacial bone regeneration. *Acta Biomater.* **2019**, *86*, 450-464.
  102. Waksman, R.; Erbel, R.; Di Mario, C.; Bartunek, J.; de Bruyne, B.; Eberli, F. R.; Erne, P.; Haude, M.; Horrigan, M.; Ilesley, C.; Böse, D.; Bonnier, H.; Koolen, J.; Lüscher, T. F.; Weissman, N. J.; PROGRESS-AMS (clinical Performance angiographic results of coronary stenting with absorbable metal stents) Investigators. Early- and long-term intravascular ultrasound and angiographic findings after bioabsorbable magnesium stent implantation in human coronary arteries. *JACC Cardiovasc Interv.* **2009**, *2*, 312-320.
  103. Cui, H. K.; Li, F. B.; Guo, Y. C.; Zhao, Y. L.; Yan, R. F.; Wang, W.; Li, Y. D.; Wang, Y. L.; Yuan, G. Y. Intermediate analysis of magnesium alloy covered stent for a lateral aneurysm model in the rabbit common carotid artery. *Eur Radiol.* **2017**, *27*, 3694-3702.
  104. Field, J. R.; Ruthenbeck, G. R. Qualitative and quantitative radiological

- measures of fracture healing. *Vet Comp Orthop Traumatol.* **2018**, *31*, 1-9.
105. Bissinger, O.; Kirschke, J. S.; Probst, F. A.; Stauber, M.; Wolff, K. D.; Haller, B.; Götz, C.; Plank, C.; Kolk, A. Micro-CT vs. whole body multirow detector CT for analysing bone regeneration in an Animal model. *PLoS One.* **2016**, *11*, e0166540.
  106. Pennington, Z.; Ehresman, J.; Lubelski, D.; Cottrill, E.; Schilling, A.; Ahmed, A. K.; Feghali, J.; Witham, T. F.; Sciubba, D. M. Assessing underlying bone quality in spine surgery patients: a narrative review of dual-energy X-ray absorptiometry (DXA) and alternatives. *Spine J.* **2021**, *21*, 321-331.
  107. Messina, C.; Sconfienza, L. M.; Bandirali, M.; Guglielmi, G.; Olivieri, F. M. Adult dual-energy X-ray absorptiometry in clinical practice: how I report it. *Semin Musculoskelet Radiol.* **2016**, *20*, 246-253.
  108. Schwarzenberg, P.; Darwiche, S.; Yoon, R. S.; Dailey, H. L. Imaging modalities to assess fracture healing. *Curr Osteoporos Rep.* **2020**, *18*, 169-179.
  109. Martín-Badosa, E.; Amblard, D.; Nuzzo, S.; Elmoutaouakkil, A.; Vico, L.; Peyrin, F. Excised bone structures in mice: imaging at three-dimensional synchrotron radiation micro CT. *Radiology.* **2003**, *229*, 921-928.
  110. Irie, M. S.; Rabelo, G. D.; Spin-Neto, R.; Dechichi, P.; Borges, J. S.; Soares, P. B. F. Use of micro-computed tomography for bone evaluation in dentistry. *Braz Dent J.* **2018**, *29*, 227-238.
  111. Só, B. B.; Silveira, F. M.; Llantada, G. S.; Jardim, L. C.; Calcagnotto, T.; Martins, M. A. T.; Martins, M. D. Effects of osteoporosis on alveolar bone repair after tooth extraction: a systematic review of preclinical studies. *Arch Oral Biol.* **2021**, *125*, 105054.
  112. Rousselle, S. D.; Wicks, J. R.; Tabb, B. C.; Tellez, A.; O'Brien, M. Histology strategies for medical implants and interventional device studies. *Toxicol Pathol.* **2019**, *47*, 235-249.
  113. Lim, S.; Kim, J. A.; Lee, T.; Lee, D.; Nam, S. H.; Lim, J.; Park, E. K. Stimulatory effects of KPR-A148 on osteoblast differentiation and bone regeneration. *Tissue Eng Regen Med.* **2019**, *16*, 405-413.
  114. Jeong, J. H.; Jin, E. S.; Kim, J. Y.; Lee, B.; Min, J.; Jeon, S. R.; Lee, M.; Choi, K. H. The effect of biocomposite screws on bone regeneration in a rat osteoporosis model. *World Neurosurg.* **2017**, *106*, 964-972.
  115. Hu, J.; Zhou, J.; Wu, J.; Chen, Q.; Du, W.; Fu, F.; Yu, H.; Yao, S.; Jin, H.; Tong, P.; Chen, D.; Wu, C.; Ruan, H. Loganin ameliorates cartilage degeneration and osteoarthritis development in an osteoarthritis mouse model through inhibition of NF- $\kappa$ B activity and pyroptosis in chondrocytes. *J Ethnopharmacol.* **2020**, *247*, 112261.
  116. Huang, Y. Combined treatment of vitamin K and teriparatide on bone metabolism and biomechanics in rats with osteoporosis. *Exp Ther Med.* **2018**, *15*, 315-319.
  117. Friedemann, M. C.; Mehta, N. A.; Jessen, S. L.; Charara, F. H.; Ginn-Hedman, A. M.; Kaulfus, C. N.; Brocklesby, B. F.; Robinson, C. B.; Jokerst, S.; Glowczwski, A.; Clubb, F. J., Jr.; Weeks, B. R. Introduction to currently applied device pathology. *Toxicol Pathol.* **2019**, *47*, 221-234.
  118. Jackson, N.; Assad, M.; Vollmer, D.; Stanley, J.; Chagnon, M. Histopathological evaluation of orthopedic medical devices: the state-of-the-art in animal Models, imaging, and histomorphometry techniques. *Toxicol Pathol.* **2019**, *47*, 280-296.
  119. Hamushan, M.; Cai, W.; Zhang, Y.; Ren, Z.; Du, J.; Zhang, S.; Zhao, C.; Cheng, P.; Zhang, X.; Shen, H.; Han, P. High-purity magnesium pin enhances bone consolidation in distraction osteogenesis via regulating Pthc protein activating Hedgehog-alternative Wnt signaling. *Bioact Mater.* **2021**, *6*, 1563-1574.
  120. Darouiche, R. O. Treatment of infections associated with surgical implants. *N Engl J Med.* **2004**, *350*, 1422-1429.
  121. Robinson, D. A.; Griffith, R. W.; Shechtman, D.; Evans, R. B.; Conzemius, M. G. In vitro antibacterial properties of magnesium metal against *Escherichia coli*, *Pseudomonas aeruginosa* and *Staphylococcus aureus*. *Acta Biomater.* **2010**, *6*, 1869-1877.
  122. Li, Y.; Liu, G.; Zhai, Z.; Liu, L.; Li, H.; Yang, K.; Tan, L.; Wan, P.; Liu, X.; Ouyang, Z.; Yu, Z.; Tang, T.; Zhu, Z.; Qu, X.; Dai, K. Antibacterial properties of magnesium in vitro and in an in vivo model of implant-associated methicillin-resistant *Staphylococcus aureus* infection. *Antimicrob Agents Chemother.* **2014**, *58*, 7586-7591.
  123. He, W.; Zhang, H.; Qiu, J. Osteogenic effects of bioabsorbable magnesium implant in rat mandibles and in vitro. *J Periodontol.* **2021**, *92*, 1181-1191.
  124. Berglund, I. S.; Jacobs, B. Y.; Allen, K. D.; Kim, S. E.; Pozzi, A.; Allen, J. B.; Manuel, M. V. Peri-implant tissue response and biodegradation performance of a Mg-1.0Ca-0.5Sr alloy in rat tibia. *Mater Sci Eng C Mater Biol Appl.* **2016**, *62*, 79-85.
  125. Tie, D.; Feyerabend, F.; Müller, W. D.; Schade, R.; Liefelth, K.; Kainer, K. U.; Willumeit, R. Antibacterial biodegradable Mg-Ag alloys. *Eur Cell Mater.* **2013**, *25*, 284-298; discussion 298.
  126. Jähn, K.; Saito, H.; Taipaleenmäki, H.; Gasser, A.; Hort, N.; Feyerabend, F.; Schlüter, H.; Rueger, J. M.; Lehmann, W.; Willumeit-Römer, R.; Hesse, E. Intramedullary Mg2Ag nails augment callus formation during fracture healing in mice. *Acta Biomater.* **2016**, *36*, 350-360.
  127. Yoshizawa, S.; Chaya, A.; Verdelis, K.; Bilodeau, E. A.; Sfeir, C. An in vivo model to assess magnesium alloys and their biological effect on human bone marrow stromal cells. *Acta Biomater.* **2015**, *28*, 234-239.
  128. Han, P.; Cheng, P.; Zhang, S.; Zhao, C.; Ni, J.; Zhang, Y.; Zhong, W.; Hou, P.; Zhang, X.; Zheng, Y.; Chai, Y. In vitro and in vivo studies on the degradation of high-purity Mg (99.99wt.%) screw with femoral intracondylar fractured rabbit model. *Biomaterials.* **2015**, *64*, 57-69.
  129. Hung, C. C.; Chaya, A.; Liu, K.; Verdelis, K.; Sfeir, C. The role of magnesium ions in bone regeneration involves the canonical Wnt signaling pathway. *Acta Biomater.* **2019**, *98*, 246-255.
  130. Wang, J.; Xu, J.; Song, B.; Chow, D. H.; Shu-Hang Yung, P.; Qin, L. Magnesium (Mg) based interference screws developed for promoting tendon graft incorporation in bone tunnel in rabbits. *Acta Biomater.* **2017**, *63*, 393-410.
  131. Li, Y.; Liu, L.; Wan, P.; Zhai, Z.; Mao, Z.; Ouyang, Z.; Yu, D.; Sun, Q.; Tan, L.; Ren, L.; Zhu, Z.; Hao, Y.; Qu, X.; Yang, K.; Dai, K. Biodegradable Mg-Cu alloy implants with antibacterial activity for the treatment of osteomyelitis: In vitro and in vivo evaluations. *Biomaterials.* **2016**, *106*, 250-263.
  132. Jiang, Y.; Wang, B.; Jia, Z.; Lu, X.; Fang, L.; Wang, K.; Ren, F. Polydopamine mediated assembly of hydroxyapatite nanoparticles and bone morphogenetic protein-2 on magnesium alloys for enhanced corrosion resistance and bone regeneration. *J Biomed Mater Res A.* **2017**, *105*, 2750-2761.
  133. Grün, N. G.; Holweg, P.; Tangl, S.; Eichler, J.; Berger, L.; van den Beucken, J.; Löffler, J. F.; Klestil, T.; Weinberg, A. M. Comparison of a resorbable magnesium implant in small and large growing-animal models. *Acta Biomater.* **2018**, *78*, 378-386.
  134. Marukawa, E.; Tamai, M.; Takahashi, Y.; Hatakeyama, I.; Sato, M.; Higuchi, Y.; Kakidachi, H.; Taniguchi, H.; Sakamoto, T.; Honda, J.; Omura, K.; Harada, H. Comparison of magnesium alloys and poly-L-lactide screws as degradable implants in a canine fracture model. *J Biomed Mater Res B Appl Biomater.* **2016**, *104*, 1282-1289.
  135. Wang, S.; Liu, Y.; Fang, D.; Shi, S. The miniature pig: a useful large

- animal model for dental and orofacial research. *Oral Dis.* **2007**, *13*, 530-537.
136. Echeverry-Rendon, M.; Allain, J. P.; Robledo, S. M.; Echeverria, F.; Harmsen, M. C. Coatings for biodegradable magnesium-based supports for therapy of vascular disease: A general view. *Mater Sci Eng C Mater Biol Appl.* **2019**, *102*, 150-163.
137. Zartner, P. A.; Schranz, D.; Mini, N.; Schneider, M. B.; Schneider, K. Acute treatment of critical vascular stenoses with a bioabsorbable magnesium scaffold in infants with CHDs. *Cardiol Young.* **2020**, *30*, 493-499.
138. Blachutzik, F.; Achenbach, S.; Tröbs, M.; Marwan, M.; Weissner, M.; Nef, H.; Schlundt, C. Effect of non-compliant balloon postdilatation on magnesium-based bioresorbable vascular scaffolds. *Catheter Cardiovasc Interv.* **2019**, *93*, 202-207.
139. Li, H.; Zhong, H.; Xu, K.; Yang, K.; Liu, J.; Zhang, B.; Zheng, F.; Xia, Y.; Tan, L.; Hong, D. Enhanced efficacy of sirolimus-eluting bioabsorbable magnesium alloy stents in the prevention of restenosis. *J Endovasc Ther.* **2011**, *18*, 407-415.
140. Bowen, P. K.; Drelich, A.; Drelich, J.; Goldman, J. Rates of in vivo (arterial) and in vitro biocorrosion for pure magnesium. *J Biomed Mater Res A.* **2015**, *103*, 341-349.
141. Waksman, R.; Pakala, R.; Kuchulakanti, P. K.; Baffour, R.; Hellinga, D.; Seabron, R.; Tio, F. O.; Wittchow, E.; Hartwig, S.; Harder, C.; Rohde, R.; Heublein, B.; Andreae, A.; Waldmann, K. H.; Haverich, A. Safety and efficacy of bioabsorbable magnesium alloy stents in porcine coronary arteries. *Catheter Cardiovasc Interv.* **2006**, *68*, 607-617; discussion 618-619.
142. Heublein, B.; Rohde, R.; Kaese, V.; Niemeyer, M.; Hartung, W.; Haverich, A. Biocorrosion of magnesium alloys: a new principle in cardiovascular implant technology? *Heart.* **2003**, *89*, 651-656.
143. Zhu, J.; Zhang, X.; Niu, J.; Shi, Y.; Zhu, Z.; Dai, D.; Chen, C.; Pei, J.; Yuan, G.; Zhang, R. Biosafety and efficacy evaluation of a biodegradable magnesium-based drug-eluting stent in porcine coronary artery. *Sci Rep.* **2021**, *11*, 7330.
144. Shi, Y.; Zhang, L.; Chen, J.; Zhang, J.; Yuan, F.; Shen, L.; Chen, C.; Pei, J.; Li, Z.; Tan, J.; Yuan, G. In vitro and in vivo degradation of rapamycin-eluting Mg-Nd-Zn-Zr alloy stents in porcine coronary arteries. *Mater Sci Eng C Mater Biol Appl.* **2017**, *80*, 1-6.
145. Zhang, J.; Li, H.; Wang, W.; Huang, H.; Pei, J.; Qu, H.; Yuan, G.; Li, Y. The degradation and transport mechanism of a Mg-Nd-Zn-Zr stent in rabbit common carotid artery: a 20-month study. *Acta Biomater.* **2018**, *69*, 372-384.
146. O'Loughlin, P. F.; Morr, S.; Bogunovic, L.; Kim, A. D.; Park, B.; Lane, J. M. Selection and development of preclinical models in fracture-healing research. *J Bone Joint Surg Am.* **2008**, *90* Suppl 1, 79-84.
147. Lang, A.; Schulz, A.; Ellinghaus, A.; Schmidt-Bleek, K. Osteotomy models - the current status on pain scoring and management in small rodents. *Lab Anim.* **2016**, *50*, 433-441.
148. Haffner-Luntzer, M.; Hankenson, K. D.; Ignatius, A.; Pfeifer, R.; Khader, B. A.; Hildebrand, F.; van Griensven, M.; Pape, H. C.; Lehmicke, M. Review of animal models of comorbidities in fracture-healing research. *J Orthop Res.* **2019**, *37*, 2491-2498.
149. Decker, S.; Reifenrath, J.; Omar, M.; Krettek, C.; Müller, C. W. Non-osteotomy and osteotomy large animal fracture models in orthopedic trauma research. *Orthop Rev (Pavia).* **2014**, *6*, 5575.
150. Sun, Y.; Wu, H.; Wang, W.; Zan, R.; Peng, H.; Zhang, S.; Zhang, X. Translational status of biomedical Mg devices in China. *Bioact Mater.* **2019**, *4*, 358-365.

Received: July 16, 2021

Revised: August 16, 2021

Accepted: September 10, 2021

Available online: September 28, 2021